Oncogene (2014) **33,** 5582–5591

www.nature.com/onc

ORIGINAL ARTICLE

ROCK has a crucial role in regulating prostate tumor growth through interaction with c-Myc

C Zhang[1,2], S Zhang[1], Z Zhang[2], J He[3], Y Xu[2] and S Liu[1]

Rho-associated kinase (ROCK) has an essential role in governing cell morphology and motility, and increased ROCK activity contributes to cancer cell invasion and metastasis. Burgeoning data suggest that ROCK is also involved in the growth regulation of tumor cells. However, thus far, the molecular mechanisms responsible for ROCK-governed tumor cell growth have not been clearly elucidated. Here we showed that inhibition of ROCK kinase activity, either by a selective ROCK inhibitor Y27632 or by specific ROCK small interfering RNA (siRNA) molecules, attenuated not only motility but also the proliferation of PC3 prostate cancer cells *in vitro* and *in vivo*. Importantly, mechanistic investigation revealed that ROCK endowed cancer cells with tumorigenic capability, mainly by targeting c-Myc. ROCK could increase the transcriptional activity of c-Myc by promoting c-Myc protein stability, and ROCK inhibition reduced c-Myc-mediated expression of mRNA targets (such as HSPC111) and microRNA targets (such as miR-17-92 cluster). We provided evidence demonstrating that ROCK1 directly interacted with and phosphorylated c-Myc, resulting in stabilization of the protein and activation of its transcriptional activity. Suppression of ROCK-c-Myc downstream molecules, such as c-Myc-regulated miR-17, also impaired tumor cell growth *in vitro* and *in vivo*. In addition, c-Myc was shown to exert a positive feedback regulation on ROCK by increasing RhoA mRNA expression. Therefore, inhibition of ROCK and its stimulated signaling might prove to be a promising strategy for restraining tumor progression in prostate cancer.

Oncogene (2014) **33,** 5582–5591; doi:10.1038/onc.2013.505; published online 9 December 2013

Keywords: ROCK; c-Myc; prostate cancer cells; proliferation; protein stability

INTRODUCTION

Rho-associated kinase (ROCK) is the fundamental downstream effector of the small GTPase Rho. ROCK is deregulated in a variety of cancers, such as prostate, breast and lung cancers, especially in advanced tumors,[1–3] and ROCK overexpression significantly contributes to metastasis by enhancing tumor cell invasion and motility.[2,4] There are two similar but distinct isoforms: ROCK1 and ROCK2 (we here refer to ROCK1 and 2 as ROCK). There is an overall 65% similarity between ROCK1 and ROCK2, particularly in the catalytic kinase domain, where there is 92% identity.[5] In spite of the structural similarities, ROCK1 and ROCK2 are differentially expressed in tissues[6] and have distinct roles in different biological settings by targeting different substrates.[7,8] ROCK1 overexpression, but not ROCK2, is often observed in cancers, and only the level of ROCK1 correlates closely with tumor progression and poor prognosis in cancer patients, including those with prostate cancer and breast cancer.[9–12] In addition, a few observations also suggest the role of ROCK in regulating tumor cell growth, such as in melanoma.[13] However, the molecular bases underlying ROCK-governed cell growth remain nearly unexplored, and the differential role of ROCK1 and ROCK2 in growth regulation still remains elusive.

Oncogene c-Myc globally reprograms cells and drives proliferation by regulating an estimated 15% of genes in the human genome.[14] Overexpression or activation of c-Myc has a decisive role in the development and progression of various cancers.[15] The phosphorylation of c-Myc at certain sites governs its activation and consequential biological functions through transcriptional activation of target genes that are necessary for cell growth, and S62 phosphorylation is necessary for its oncogenic activity.[16] Previous studies have revealed that ROCK has a crucial role in stabilizing c-Myc protein via S62 phosphorylation in RhoA-transformed kidney epithelial cells[17] and breast cancer cells.[10] However, whether ROCK directly phosphorylates c-Myc (that is, a direct physical interaction between ROCK and c-Myc) and whether there is a feedback regulation of c-Myc on ROCK remain to be determined.

In the current study, we gained insights into the regulation of ROCK on prostate cancer growth: ROCK increased the transcriptional activity of c-Myc by promoting c-Myc protein stability through phosphorylation and subsequent nuclear transportation. We also verified a novel mechanism of a positive feedback regulation of c-Myc on ROCK through transcriptional upregulation of RhoA. Inhibition of ROCK activity or downstream ROCK-mediated events appears to be a promising strategy for restraining prostate tumor progression.

RESULTS

ROCK inhibition reduced cell motility and growth *in vitro* and *in vivo*

To shed light on the role of ROCK in regulating prostate cancer cell growth and progression, we inhibited ROCK kinase activity in PC3

[1]State Key Laboratory of Environmental Chemistry and Ecotoxicology, Research Center for Eco-Environmental Sciences, Chinese Academy of Sciences, Beijing, China; [2]Department of Urology, Second Hospital of Tianjin Medical University, Tianjin Institute of Urology, Tianjin, China and [3]Department of Biomedical Engineering, Tufts University, Medford, MA, USA. Correspondence: Professor S Liu, State Key Laboratory of Environmental Chemistry and Ecotoxicology, Research Center for Eco-Environmental Sciences, Chinese Academy of Sciences, Beijing 100085, China or Professor Y Xu, Department of Urology, Second Hospital of Tianjin Medical University, Tianjin Institute of Urology, Tianjin 300211, China.
E-mail: sjliu@rcees.ac.cn or xuyong8816@sina.com
Received 25 June 2013; revised 23 October 2013; accepted 23 October 2013; published online 9 December 2013

cells using a selective inhibitor, Y27632, and specific siRNA molecules. ROCK activity was reduced by 39% and 68% upon treatment with Y27632 at 10 and 20 μM for 48 h, respectively, ($P<0.05$, Figure 1a), resulting in a significant reduction in phosphorylated myosin light chain (Figure 1a), a necessary substrate of ROCK. As myosin light chain phosphorylation increases the assembly of filamentous myosin heavy chains and enhances the binding between myosin and filamentous actin (F-actin),[5] ROCK inhibition with Y27632 led to a significant reduction in stress fiber formation as reflected by the decreased intensity of actin meshwork and condensed cellular morphology (Figure 1b), consistent with previous observations.[10] Cell motility was restrained by 67% and 78% as assessed with cytodex beads and the transwell assay, respectively, ($P<0.05$, Supplementary Figures 1A and B). In addition, Y27632 treatment diminished cell growth of PC3 cells treated with Y27632 at 20 μM for 48 h by 24% in the MTT proliferation assay and by 30% in the BrdU incorporation assay ($P<0.05$, Figure 1c). The attenuation in cell growth was also reflected in the colony formation assay: the average size of colonies in the group treated with Y27632 was significantly diminished ($P<0.05$, Supplementary Figure 1c). In the *in vivo* experiments, all mice developed tumors at the injected sites. In agreement with the *in vitro* observation, ROCK inhibition *in vivo* exerted a robust inhibitory effect on tumor growth in mice inoculated with PC3 cells, as the growth of tumor volume over the course of time and the final tumor weight were reduced by >20% in mice treated with an intravenous injection of Y27632 compared with control mice ($P<0.05$, Figure 1d). Tumor metastases were also closely examined in these mice. As shown in Supplementary Figure 2, the occurrence of tumor lung metastases was 30% (3 out of 10 mice) in control mice; however, no lung metastasis (0 out of 10 mice) was observed in mice treated with Y27632 (Supplementary Figure 2). In addition, the overall health conditions of the mice administrated Y27632 were not affected. As shown in Supplementary Figure 3, no body weight loss was found. Moreover, no abnormal activity or diets were observed. These observations suggested that the ROCK inhibitor administration at the current dose rendered no gross toxicity to mice, which was similar to previous reports.[10,18,19]

Similar results for kinase activity, myosin light chain phosphorylation, cell motility and growth were also observed in cells transfected with ROCK-specific siRNA molecules compared with the scrambled control and blank control ($P<0.05$, Figures 2 and 3a). Moreover, cell cycle progression was impeded in PC3 cells treated with Y27632. The percentage of G1 phase increased to 72% in cells treated with Y27632 at 20 μM for 48 h with a corresponding reduction in the percentages of the S phase and the G2/M phase, in comparison with 58% for the G1 phase in control cells (Figure 3b, $P<0.05$). It should be noted that ROCK inhibition had little influence on cell death, as Y27632 treatment did not induce apoptosis or necrosis as determined by fluorescence-activated cell sorting analysis using fluorescein isothiocyanate-annexin V and propidium iodide staining (data not shown). Taken together, these data reveal an important role for ROCK in regulating prostate cancer cell motility and proliferation.

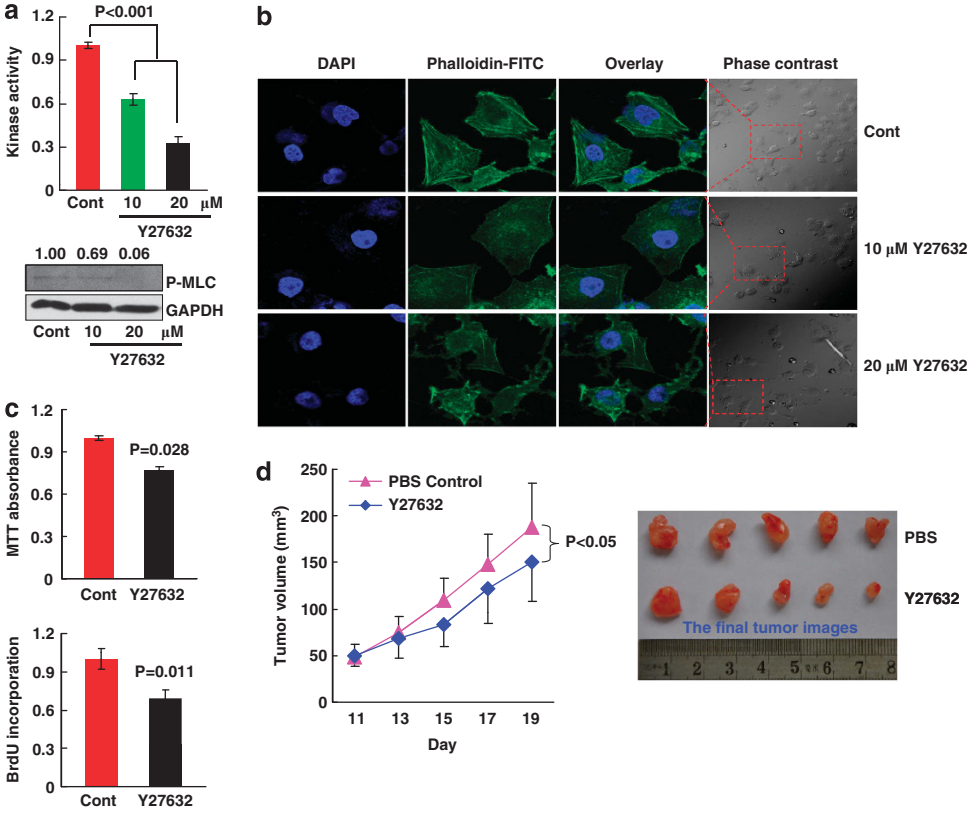

Figure 1. ROCK inhibition by Y27632 reduced cell motility and growth in PC3 cells. (**a**) The relative ROCK kinase activity ($n=3$) and the phosphorylated myosin light chain (p-MLC) protein level reflected by western blot analysis in PC3 cells with or without Y27632 treatment at 10 or 20 μM for 48 h. (**b**) Confocal imaging of F-actin stained with fluorescein isothiocyanate (FITC)-conjugated phalloidin in PC3 cells upon exposure to Y27632 at 10 or 20 μM for 24 h. The F-actin filaments are shown in green and the cell nuclei are shown in blue by counterstaining with 4,6-diamidino-2-phenylindole (DAPI). Original magnification, × 400 for enlarged images of fluorescent staining and × 40 for bright-field images. (**c**) Cell proliferation assessed with the MTT method and the BrdU incorporation method in PC3 cells treated with Y27632 at 20 μM for 48 h. (**d**) The tumor growth curve in mice inoculated with PC3 cells upon intravenous injection of Y27632 ($n=10$). The representative image of tumors from Y27632-treated mice and the control mice.

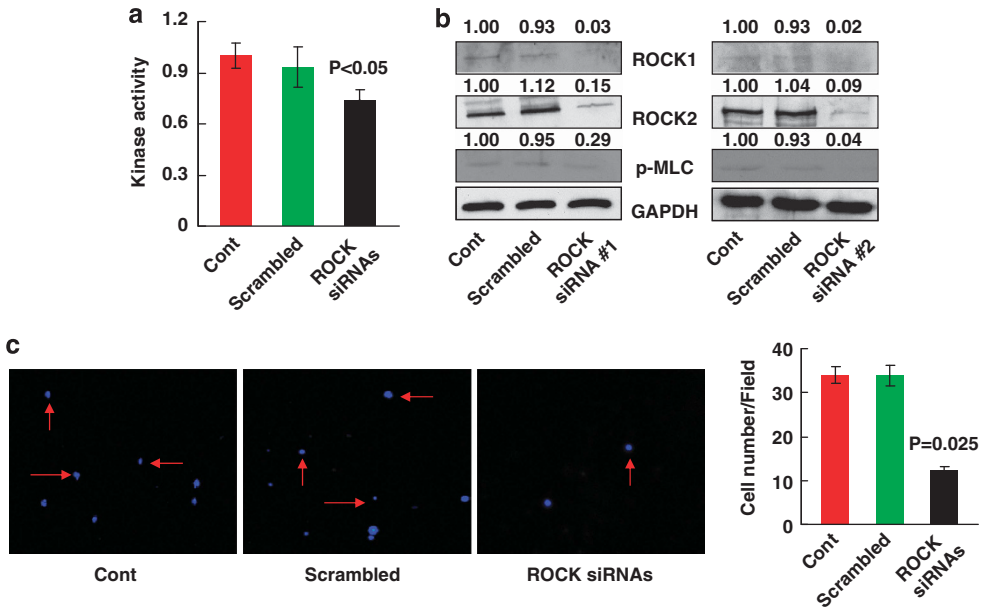

Figure 2. Migration of PC3 cells upon transfection with ROCK siRNA molecules. (**a**) The relative ROCK kinase activity in PC3 cells transfected with ROCK siRNA molecules for 48 h ($n = 3$). (**b**) The phosphorylated myosin light chain (p-MLC) protein level in PC3 cells transfected with two different sets of ROCK siRNA molecules (siRNA #1 and siRNA #2). (**c**) Transwell migration assay for cell motility upon ROCK silencing with siRNAs in PC3 cells. Representative images from the transwell migration assay for PC3 cells transfected with siRNAs; the numbers of transmigrated cells were quantified ($n = 6$).

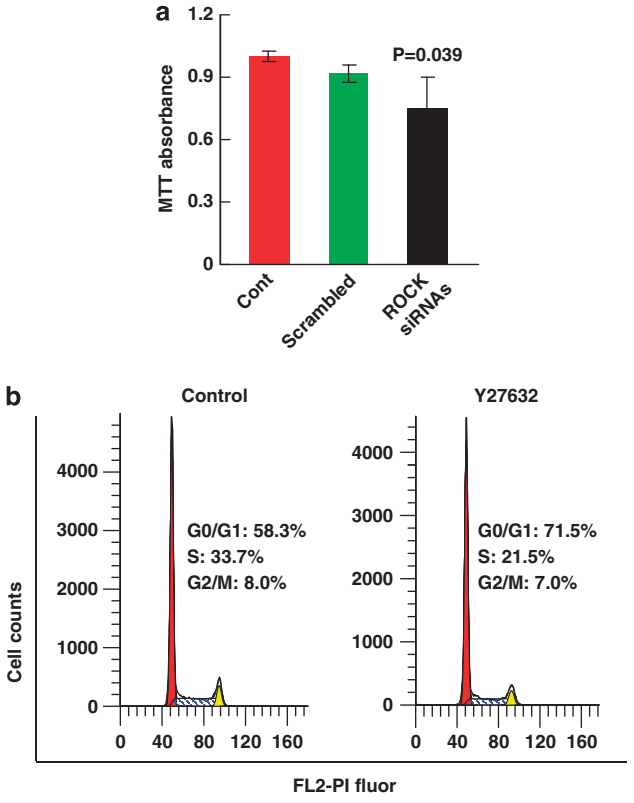

Figure 3. Proliferation of PC3 cells upon ROCK inhibition. (**a**) Cell proliferation was assessed with the MTT method in PC3 cells transfected with ROCK siRNA molecules ($n = 6$). (**b**) Cell cycle progression assessment for PC3 cells treated with Y27632 at 20 μM for 48 h. Representative profiles of DNA content measured by fluorescence-activated cell sorting analysis are shown with the percentages of various phases.

ROCK enhanced the stability and the transcriptional activity of c-Myc

To elucidate the mechanisms by which ROCK modulates tumor growth, we looked into the downstream targets of ROCK. In addition to motor proteins, ROCK was suggested to target the oncogene c-Myc.[17,20] We thus investigated the c-Myc level and the c-Myc downstream targets upon ROCK inhibition in PC3 cells. Upon attenuation of ROCK activity with siRNAs for 48 h, the level of c-Myc total protein was greatly decreased (Figure 4a). Moreover, we used an antibody to detect phosphorylated c-Myc (p-c-Myc), which recognizes c-Myc protein singly or doubly phosphorylated at either S62 or T58, or both. Consistent with previous studies,[10,17] a significant reduction in p-c-Myc was observed in cells transfected with ROCK-siRNAs (Figure 4a). Similar to siRNA-mediated knockdown of ROCK, a robust reduction in c-Myc and p-c-Myc was observed upon ROCK inhibition with Y27632 at 10 and 20 μM for 48 h (Figure 4b). To substantiate this finding, we treated cells with 20 μM Y27632 at different time points, from 12 to 36 h; significantly reduced c-Myc and p-c-Myc were demonstrated after 24-h treatment (Figure 4c). In parallel to these findings, increased kinase activity of c-Jun N-terminal kinase or apoptosis signal-regulating kinase 1 has been demonstrated to stabilize c-Myc in a S62 phosphorylation-dependent manner.[21–23] These results verified an important role of ROCK-mediated S62 phosphorylation in stabilizing c-Myc.

The activated form of c-Myc (after S62 phosphorylation) appears necessary for the stability of the c-Myc protein and for c-Myc-mediated cell cycle progression and tumorigenesis.[16,24–26] S62-phosphorylated c-Myc would activate a set of target genes that facilitate cell cycle progression.[16] Upon ROCK diminishment by siRNAs or by the ROCK inhibitor, a direct transcriptional target of c-Myc,[27] HSPC111, was significantly decreased (Figures 4a and b), confirming the regulation of ROCK on c-Myc activity. HSPC111 is overexpressed in breast cancers, and it has a role in promoting cell growth through modulation of ribosomal RNA synthesis and ribosomal assembly.[27]

To substantiate the role of S62 phosphorylation in enhancing c-Myc's transcriptional activity, we mutated S62 into Ala (S62A) in

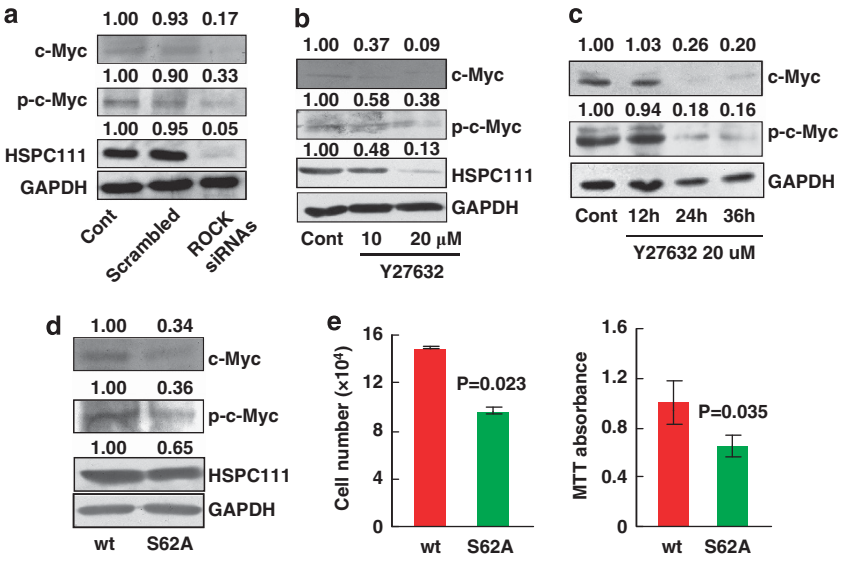

Figure 4. ROCK enhanced the stability and transcriptional activity of c-Myc. (**a**) Western bolt analyses of c-Myc, p-c-Myc and HSPC111 in PC3 cells transfected with ROCK siRNA molecules for 48 h. (**b**) Western bolt analyses of c-Myc, p-c-Myc and HSPC111 in PC3 cells upon exposure to Y27632 at 10 or 20 μM for 48 h. (**c**) Western bolt analyses for c-Myc and p-c-Myc in PC3 cells treated with Y27632 at 20 μM at 12, 24 and 36 h. (**d**) Western bolt analyses of p-c-Myc, c-Myc and HSPC111 in PC3 cells transfected with wt c-Myc plasmid or S62A c-Myc plasmid (S62A) for 48 h. (**e**) Proliferation of PC3 cells upon transfection of wt c-Myc plasmid or S62A c-Myc plasmid, determined by the cell counting and the MTT method ($n = 4–6$).

a c-Myc expression construct with the site-directed mutagenesis method, and assessed the p-c-Myc level using specific antibody without cross-reactivity to non-phosphorylated c-Myc.[17] Upon S62A mutation, we observed a significant reduction in p-c-Myc level, total c-Myc level and HSPC111 level (Figure 4d), indicating reduced protein stability and diminished ability of c-Myc in transcription because of the absence of S62 phosphorylation. Cell growth was subsequently diminished by >35% in cells with S62A mutation, as evidenced by cell number counting and the MTT assay (Figure 4e). Together, our results suggested that S62 phosphorylation of c-Myc promoted its protein stability and transcriptional activity, which is necessary for cell growth.

Blockade of miR-17 restrained tumor growth *in vitro* and *in vivo*

In addition to mRNAs, a number of microRNAs (miRNAs) are also regulated by c-Myc. The miR-17-92 cluster is directly transcribed by c-Myc (Figure 5a), and it has been recognized as an oncogene in human cancers.[28] Owing to c-Myc reduction resulting from ROCK inhibition, the miR-17-92 expression was greatly reduced (Figure 5a). As expected, an established target of miR-17,[29] the type II transforming growth factor β receptor (TβRII), was elevated because of the decrease in the miR-17 level on treatment with Y27632 (Figure 5a). Among the miRNAs within this cluster, miR-17, miR-19a, miR-19b-1 and miR-92a-1 were upregulated 1–1.5-fold in prostate tumors compared with normal tissues (Figures 5b and c), suggesting a critically important role of these miRNAs in tumorigenesis of prostate cancer. miR-17 has been postulated to be involved in the regulation of cell growth, and elevated miR-17 enhances cell proliferation and tumor growth by targeting a few mRNA targets, such as TβRII.[29] The effect of miR-17 blockade on tumor growth of prostate cancer has not been investigated thus far. To this end, we blocked endogenous miR-17 with anti-miR-17 molecules in PC3 cells. As shown in Figure 5d, cell growth was significantly decreased, as reflected by the cell number counting and the MTT assay ($P < 0.05$). In agreement with the *in vitro* results, tumor growth was reduced by treatment with the anti-miR-17 molecules *in vivo*, as evidenced by the difference in tumor volumes over the course of time between the anti-miR-17 group and the scrambled control group ($P < 0.05$, Figure 5e). The final tumor weight was also reduced in the anti-miR-17-treated mice compared with controls ($P < 0.05$, data not shown). To assess the efficacy and stability of the anti-miR-17 molecules *in vivo*, we eventually performed western blotting to determine the level of the miR-17 target TβRII. As shown in Figure 5f, the TβRII concentration was markedly elevated by approximately twofold ($P < 0.05$) in the tumors administrated with anti-miR-17, compared with that in tumors treated with the scrambled molecules. These results showed that anti-miR-17 molecules were a type of efficient, specific and stable silencer for endogenous miR-17 *in vivo*. Collectively, our data recognized an important role of miR-17 in modulating the tumor growth of prostate cancer.

ROCK directly targeted c-Myc protein

Although the regulation of c-Myc protein stability by ROCK is recognized as described above, it is unclear whether ROCK can phosphorylate c-Myc directly or through an intermediate kinase, and whether c-Myc phosphorylation by ROCK is necessary for its increased oncogenic activity. We then studied the interaction between c-Myc and ROCK with Co-immunoprecipitation and glutathione *S*-transferase (GST)-pulldown assays. As shown in Figure 6a, ROCK1 bound to c-Myc directly, as demonstrated by the Co-immunoprecipitation assay performed in PC3 cells, but not ROCK2. This interaction was confirmed by the GST-pulldown assay (Figure 6b). To confirm the interaction between ROCK1 and c-Myc, we used a second cell line called the breast cancer MDA-MB-231. Similar results were also observed for MDA-MB-231 cells, as shown in Figure 6c. These results are in agreement with findings of a positive correlation of ROCK1 (but not of ROCK2) with poor prognosis and overall survival in cancer patients, and support the role of ROCK1 in modulating tumor malignancy.[9–11]

To assess whether c-Myc phosphorylation by ROCK results in an enhanced oncogenic activity of c-Myc, we examined c-Myc's nuclear localization and subsequent oncogenic activity. ROCK inhibition by Y27632 significantly reduced the p-c-Myc levels not only in the cytoplasm but also in the nuclei (Figure 6d). Immunohistochemical analysis further confirmed this alteration

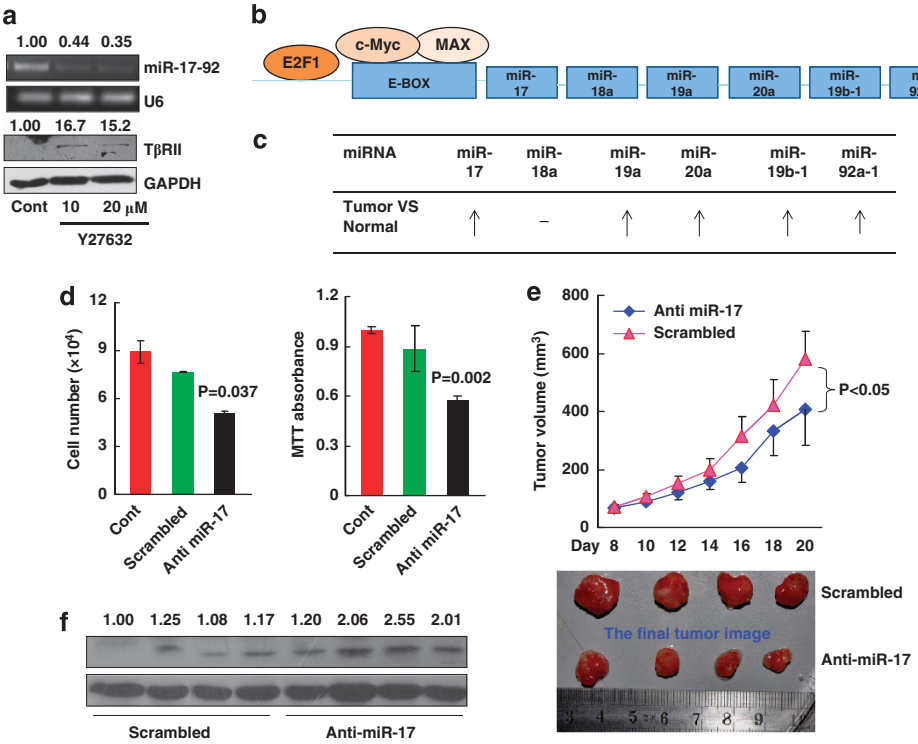

Figure 5. Blockade of miR-17 restrained tumor growth *in vitro* and *in vivo*. (**a**) The RT–PCR analysis of the miR-17–92 cluster expression and western bolt analysis of the TβRII level in PC3 cells upon exposure to Y27632 at 20 μM for 48 h with U6 or glyceraldehyde 3-phosphate dehydrogenase used as loading control, respectively. (**b**) A schematic representation of c-Myc-regulated miR-17–92 cluster. (**c**) The expression changes within the miR-17–92 cluster in the prostate tumors compared with matched normal tissues. ↑indicates 1–1.5-fold increase. (**d**) Cell growth of PC3 cells upon blockade with anti-miR-17 molecules assessed with the cell counting and the MTT method ($n = 4$–6). (**e**) The tumor growth curves in mice that harbored tumor implants derived from PC3 cells with or without intratumoral administration of anti-miR-17 molecules ($n = 10$). The lower panel shows a representative image of tumors from mice injected with anti-miR-17 molecules, as well as control mice. (**f**) Western blot analysis of TβRII concentrations in tumors with or without administration of anti-miR-17 molecules.

in p-c-Myc levels in the cytosolic and nuclear compartments (Figure 6e). As a result, the transcriptional activity of c-Myc was repressed as the concentration of its direct target HSPC111 was diminished (Figure 4); the proliferative capability of PC3 cells was accordingly abolished (Figures 1–3).

A feedback regulation of c-Myc on the RhoA-ROCK axis

To date, the possible feedback regulation of c-Myc on ROCK signaling has not been explored. A recent report suggested a potential regulation of c-Myc on RhoA at the transcriptional level to drive cell growth and migration for 293T and MDA-MB-231 cells.[20] As RhoA is a principal small GTPase and a direct upstream regulator of ROCK, we studied the relationship between c-Myc and RhoA in PC3 cells. We treated PC3 cells with a c-Myc inhibitor 10058-F4 for 24 h, and then assessed the transcriptional activity of c-Myc. A significant reduction of HSPC111 mRNA expression by 72% was observed in PC3 cells upon c-Myc repression ($P < 0.05$, Figure 7a), suggesting a robust inhibition of c-Myc activity by the c-Myc inhibitor. A reduction in RhoA mRNA expression by 30% was also observed ($P < 0.05$, Figure 7a). To clearly delineate the RhoA-ROCK-c-Myc pathway, we treated PC3 cells with three inhibitors: the RhoA inhibitor CT04, the ROCK inhibitor Y27632 and the c-Myc inhibitor 10058-F4. The ROCK inhibitor significantly reduced the levels of c-Myc, p-c-Myc, phosphorylated myosin light chain and HSPC111 (Figure 7b), in agreement with the results delineated in Figure 4. Similar observations were demonstrated when cells were treated with the RhoA inhibitor (Figure 7b), thus confirming a direct regulation of RhoA on ROCK.[5] More importantly, the RhoA protein level was markedly reduced upon treatment with the c-Myc inhibitor (Figure 7b), which was consistent with the alteration at the mRNA level (Figure 7b). As expected, when treated with the c-Myc inhibitor, decreases in phosphorylated myosin light chain, p-c-Myc and HSPC111 were also demonstrated (Figure 7b). Moreover, RhoA-ROCK-c-Myc signaling was assessed in MDA-MB-231 cells. As shown in Figure 7c, the molecular cascade of RhoA-ROCK-c-Myc including the feedback regulation was confirmed in MDA-MB-231 cells. Parallel to the changes at different points along the RhoA-ROCK-c-Myc pathway, corresponding changes in the proliferative capability of cells were observed (Figure 7d). The ROCK inhibitor and the RhoA inhibitor impeded cell growth ($P < 0.05$), and to a greater extent the c-Myc inhibitor diminished cell growth ($P < 0.01$; Figure 7d). These data indicated a role for RhoA-ROCK-c-Myc signaling in regulating the oncogenic properties of PC3 cells, and also revealed a positive feedback regulation of c-Myc on the expression of RhoA.

DISCUSSION

ROCK signaling is frequently upregulated in human cancers. Previous studies have demonstrated an important role of ROCK in the metastatic process by facilitating cancer cell invasion and migration.[5] Meanwhile, increasing evidence suggests that ROCK signaling is also involved in regulating tumor growth.[30] A recent study indicates that ROCK provokes tumor growth by modulating extracellular matrix deposition, remodeling and tissue stiffness.[31] In addition, previous studies suggest that ROCK activation leads to S62 phosphorylation and the consequential stabilization of c-Myc in Ras-expressing cells and breast cancer cells.[10,17] Clinical studies

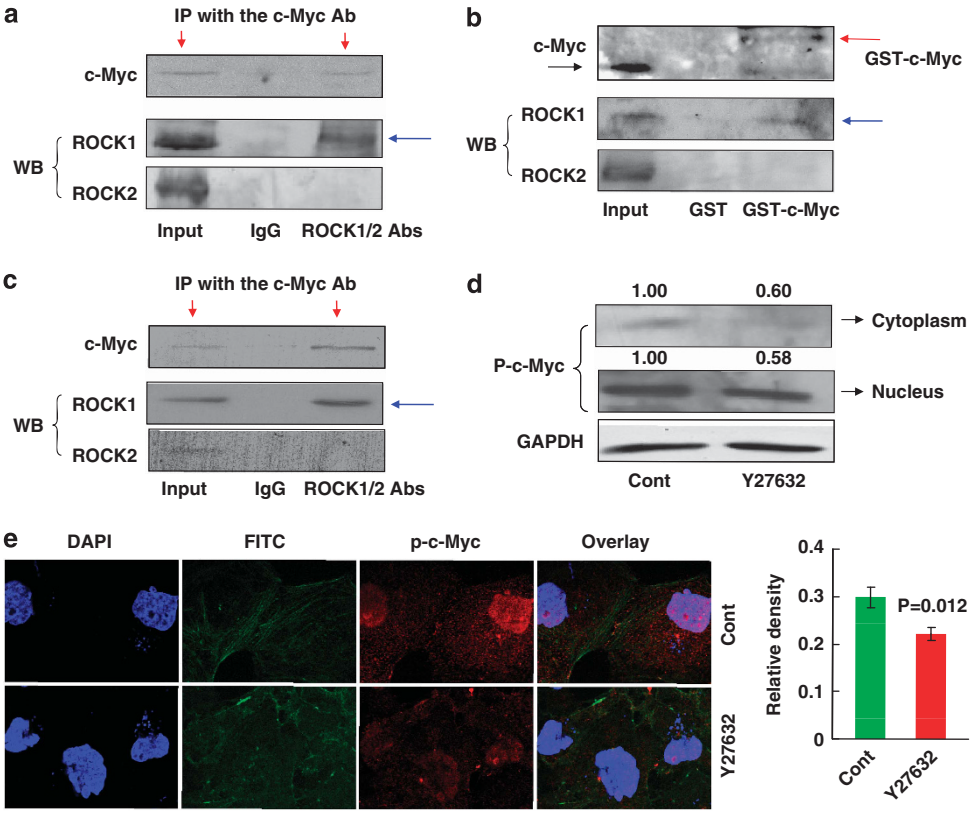

Figure 6. The interaction between c-Myc and ROCK. (**a**) The Co-immunoprecipitation assessment indicated a direct interaction between c-Myc and ROCK1 in PC3 cells. PC3 cell lysates were immunoprecipitated with anti-c-Myc Ab, and co-immunoprecipitated proteins were examined against anti-ROCK1 or anti-ROCK2 Ab using western blot analysis. The red arrows indicate c-Myc protein in the IP assessments and the blue arrow indicates the existence of ROCK1 in the co-immunoprecipitated proteins as evidenced by the western blot analysis. (**b**) The GST-pulldown assay confirmed the interaction between c-Myc and ROCK1. The GST-tagged c-Myc protein was immobilized and purified on resin and then incubated with PC3 cell lysates. The black arrow indicates the positive control of c-Myc from PC3 cell lysates and the red arrow indicates the GST-c-Myc fusion protein characterized by western blot analysis with the c-Myc Ab. The blue arrow indicates the existence of ROCK1 in the GST-c-Myc-bound proteins reflected by the western blot analysis. (**c**) The Co-immunoprecipitation assessment recognized a direct interaction between c-Myc and ROCK1 in MDA-MB-231 cells. (**d**) Western blot analysis of p-c-Myc in the cytoplasm and nucleus. PC3 cells were treated with 20 μM Y27632 for 48 h, and the cytosolic and nuclear proteins were then extracted for the western blot analysis. (**e**) Immunofluorescent staining of p-c-Myc in PC3 cells treated with Y27632. PC3 cells were treated with Y27632 at 20 μM for 48 h; then confocal images of immunofluorescent staining of p-c-Myc were taken. p-c-Myc is shown in red with F-actin in green (fluorescein isothiocyanate (FITC)-conjugated phalloidin) and nuclei in blue (4,6-diamidino-2-phenylindole (DAPI)). The bar graph shows the quantified data of the immunofluorescent staining of p-c-Myc. Original magnification, × 400.

reveal that c-Myc's localization in nuclei is associated with an aggressive phenotype and poor progression in B-lymphoma patients.[32,33] In the present study, we demonstrate overall that ROCK governs tumor growth by enhancing c-Myc activity through regulation of protein stability and nuclear translocation in PC3 prostate cancer cells.

A rapid rate of c-Myc protein degradation (half-life of only 20–30 min in rapidly dividing cells) allows tight regulation on c-Myc activity. S62 phosphorylation is necessary for the stability of the c-Myc protein and its activity.[16] Previous studies demonstrate that mutation of S62 causes a twofold decrease in Gal4-c-Myc activity;[34] correspondingly, increasing S62 phosphorylation results in a >4-fold enhancement in Gal4-c-Myc activity.[35] In the current study, we demonstrate that ROCK inhibition reduces c-Myc protein stability by repressing its S62 phosphorylation and that the mutation of S62 to Ala diminishes the transcriptional activity of c-Myc. In support of this finding, S62 phosphorylation by c-Jun N-terminal kinase or apoptosis signal-regulating kinase 1 kinase also results in enhanced stability of c-Myc.[21–23] Moreover, a direct interaction between ROCK1 and c-Myc is verified by the Co-immunoprecipitation and GST-pulldown assays; however, ROCK2 might not interact with c-Myc or at least the interaction is rather weak, which could not be characterized with the techniques employed in the current study. These findings stress the important contribution of upregulated ROCK signaling to tumorigenesis by affecting c-Myc protein stability and also support a positive correlation of ROCK1 (but not ROCK2) to poor prognosis and overall survival in cancer patients.[9–11] Regarding the regulation of c-Myc protein stability, phosphorylation of c-Myc at conserved residues S62 and T58 has an important role in this process. Phosphorylation of S62 could transiently increase c-Myc stability, whereas T58 phosphorylation is closely correlated with the degradation of c-Myc.[16] In fact, the actual degradation of c-Myc is triggered by a ubiquitin-mediated process, and the ubiquitination of c-Myc is tightly dependent on its phosphorylation.[36] FBW7 (a ubiquitin E3 ligase) and Usp28 (a ubiquitin-specific protease) synergistically regulate c-Myc stability through ubiquitin-mediated degradation.[37–39] Moreover, we identified a novel positive feedback regulation of c-Myc on RhoA/ROCK signaling by directly transcribing RhoA mRNA in PC3 cells, similar to results obtained in 293T and MDA-MB-231 breast cancer cells.[20]

To summarize, we decipher here a novel mechanism by which ROCK governs prostate tumor growth by enhancing c-Myc activity through the regulation of protein stability and nuclear translocation.

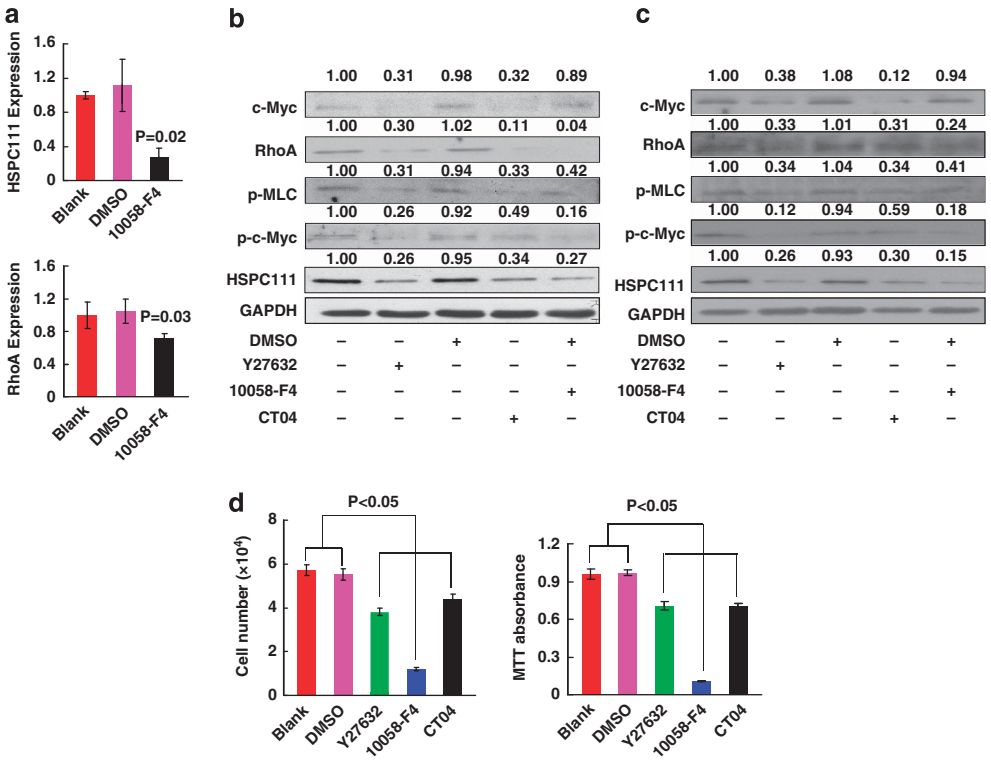

Figure 7. A feedback regulation of c-Myc on the RhoA-ROCK axis. (**a**) The transcriptional activity of c-Myc upon treatment with 10058-F4. Quantitative reverse transcriptase (qRT)–PCR showed RhoA and HSPC111 mRNA expression in PC3 cells treated with 100 μM c-Myc inhibitor 10058-F4 for 24 h, and in the blank control cells and the vehicle (DMSO) control cells ($n = 3$–4). (**b**) Western blot analyses of proteins along the RhoA-ROCK-c-Myc signaling in PC3 cells. PC3 cells were treated with 20 μM Y27632 or 100 μM 10058-F4 for 24 h, or with 1.0 μg/ml CT04 for 6 h. Total protein extracts were subject to western blot analyses for RhoA, c-Myc, p-c-Myc, HSPC111 and phosphorylated myosin light chain (p-MLC). (**c**) Western blot analyses of proteins in MDA-MB-231 cells with the same treatments as described in (**b**). (**d**) Cell growth of PC3 cells was assessed by cell number counting and the MTT method. PC3 cells were treated with 20 μM Y27632 or 100 μM 10058-F4 for 24 h, or with 1.0 μg/ml CT04 for 6 h; cell proliferation was then determined ($n = 8$–10). DMSO (0.5%) served as the vehicle control here.

Mechanistic data reveal that ROCK1 directly interacts with and stabilizes the c-Myc protein, but ROCK2 might not. In addition, c-Myc further modulates ROCK activity via a positive feedback regulation of RhoA at the transcriptional level. Inhibition of ROCK activity or ROCK-mediated downstream substrates suppresses cancer cell growth *in vitro* and *in vivo* for PC3 cells. This work together highlights a crucial role of ROCK signaling in cancer progression through modulation of c-Myc activity as illustrated in Figure 8. Thus, inhibition of ROCK signaling might represent a prospective approach toward limiting prostate tumor progression.

MATERIALS AND METHODS

Cell culture

The human prostate cancer PC3 cell line and the breast cancer MDA-MB-231 cell line were purchased from the Shanghai Cell Bank of Type Culture Collection of the Chinese Academy of Sciences, Shanghai, China. The cells were cultured in RPMI-1640 medium with 10% fetal calf serum and penicillin–streptomycin (100 units/ml) at 37 °C with 5% CO_2.

Animal experiments

All animal care and surgical procedures were approved by the Animal Ethics Committee at RCEES, CAS. Six-week-old immunodeficient (BALB/c nude) male mice were maintained in-house under aseptic sterile conditions. Surgeries were performed under sterile conditions and the mice received antibiotics (Gentamycin) in drinking water up to 2 weeks following the surgical procedures. For the tumor formation assay, 9.0×10^5 PC3 cells were inoculated subcutaneously and bilaterally underneath the back close to the forelimbs. The cells were injected in 1:2 diluted matrigel (BD Biosciences, San Jose, CA, USA), sterile phosphate-buffered saline (PBS), using a Hamilton syringe. From the first day after cell injection, one group of mice received a selective ROCK inhibitor, Y27632 (Sigma, St Louis, MO, USA), at 4 mg/kg body weight in 100 μl PBS, injected through the tail vein (intravenous), every other day for 20 days and the control mice received only PBS. Tumor size was closely monitored with a vernier caliper and calculated according to the formula $1/2 \times L \times W \times H$ periodically. Mice were euthanized when tumors reached a size of 1.0 cm^3. Tumors were separated, and a proportion of tumor tissue was fixed in 10% formaldehyde and some were stored at −80 °C for future analyses.

To assess the inhibitory effect on tumor growth by anti-miR-17, we established a mouse model of prostate cancer with tumor tissue implantation. The experimental setup was similar to our previous method.[40] Briefly, tumors derived from PC3 cells were grown on nude mice, and tumors with a volume >1 cm^3 were separated and cut into cylindrical fragments. Tumor fragments were implanted into the back behind the right forelimbs of recipient mice. Two weeks later when tumors reached 75 mm^3, anti-miR-17 or scrambled control RNA molecules in 50 μl PBS (2 mg/ml in PBS) were injected intratumorally every other day for 20 days. The anti-miR-17 and scrambled RNAs were synthesized as previously described.[28,41] The sequence of anti-miR-17 molecules was 5′-$a_s c_s$uaccugcacuguaagc $acu_s u_s u_s g_s$-Chol 3′ and the sequence of scrambled RNA molecules was 5′-$u_s a_s$cauacuucuuuacauu$_s c_s c_s a_s$-Chol 3′. Lower case letters refer to 2′-O-methyl-modified nucleotides. Subscript 's' represents a phosphorothioate linkage. 'Chol' refers to the linked cholesterol.

Gene expression analysis of the miR-17–92 cluster in prostate cancer

A publically available data set was used to assess the miR-17–92 expression in prostate tumors.[42] The data set was generated using the Agilent microRNA V2 arrays (Agilent Technologies, Inc., Santa Clara, CA, USA) from 218 tumor samples and 149 matched normal adjacent tissues. The

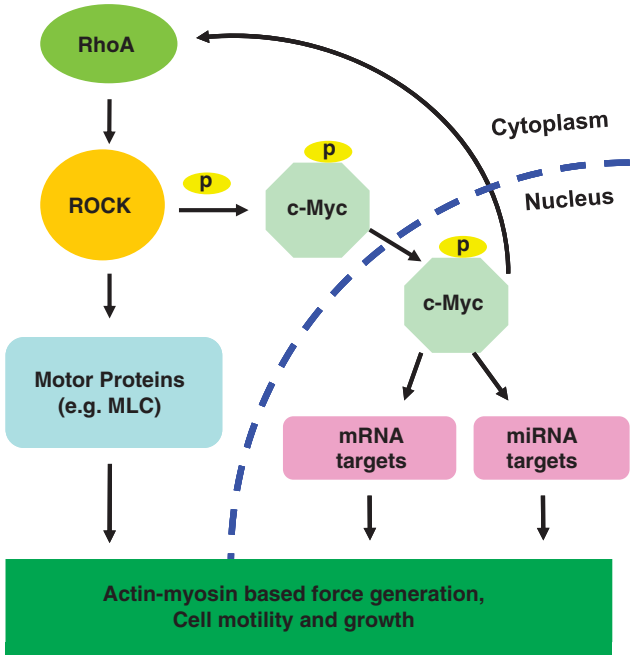

Figure 8. A schematic diagram describing a model responsible for the RhoA-ROCK-c-Myc signaling in facilitating tumor cell motility and growth. ROCK endows cancer cells with metastatic and proliferative capabilities (1) by targeting motor proteins and (2) by enhancing c-Myc activity through protein stability and nuclear translocation. Increased c-Myc activity provokes cell growth and exerts a stimulatory effect on RhoA expression via a feedback loop.

normalized miRNA expression data were obtained from the GEO database (accession number, GSE 21031).

Western blot analysis

Cells were harvested into lysis buffer (Solarbio, Beijing, China) after washing with PBS. The cytoplasmic and nuclear protein contents were extracted with a ProteoJET Cytoplasmic and Nuclear Protein Extraction Kit (Thermo Fisher Scientific, Rockford, IL, USA) according to the manufacturer's instructions. Protein concentrations were determined, and equal amounts of protein (30–50 μg/sample) were subjected to 8–12% sodium dodecyl sulfate–polyacrylamide gel electrophoresis and western blot analysis as described previously.[43] Antibodies used in the current study are described in Supplementary Table 1.

Immunoprecipitation

Cells were lysed with the mammalian protein extraction reagent (CWBIO, Beijing, China) and incubated with 2 μg c-Myc antibody or normal mouse immunoglobulin G. Thereafter, immunoprecipitates were collected with Gamma-Bind A Sepharose beads (GE Healthcare, Uppsala, Sweden). Immunoprecipitated proteins were then subjected to sodium dodecyl sulfate–polyacrylamide gel electrophoresis and western blot analysis.

GST-pulldown assay

Full-length c-Myc complementary DNA was cloned from PC3 cells and inserted into the pGEX-6p-1 vector. The recombinant construct was transformed into Rosetta (DE3)-competent cells. The expression of GST-tagged c-Myc protein was induced with 1.0 mM isopropyl-D-thiogalacto-pyranoside and then purified with GST Sefinose Resin according to the manufacturer's instructions (Sangon Biotech, Shanghai, China). PC3 cell proteins were extracted and dialyzed against binding buffer (PBS with 0.5% Triton X-100 and 0.1 mg/ml bovine serum albumin) overnight at 4 °C. The dialyzed proteins were then incubated overnight with the GST-c-Myc fusion protein in GST-tubes at 4 °C with rotation. GST-tubes were washed three times with the binding buffer, and the bound proteins were eluted and assessed by western blot analysis.

Cell proliferation assay, colony formation assay and cell cycle assessment

Cell growth was determined by the MTT assay, cell counting and the BrdU incorporation assay. In brief, PC3 cells were serum-starved overnight and then seeded at a concentration of 5.0×10^4 cells/well in 100 μl culture medium with 1% FBS in the absence or presence of 10 μM or 20 μM Y27632 for 48 h, 100 μM c-Myc inhibitor 10058-F4 (Sigma) for 24 h or 1.0 μg/ml RhoA inhibitor CT04 (Cytoskeleton, Inc., Denver, CO, USA) for 6 h. Then cell growth was assessed following the manufacturer's instructions. For the colony formation assay, a single-cell suspension at a density of 5 cells/ml was prepared and inoculated into a 96-well plate at 100 μl per well. At 4 h after cell inoculation, all 96 wells were checked under a microscope and the wells with only one cell were selected for follow-up observation. Cells were cultured with 10% fetal calf serum and observed for up to 10 days. The size of colonies was recorded under a microscope.

Cell cycle progression was determined by fluorescence-activated cell sorting analysis with propidium iodide staining. PC3 cells were serum-starved overnight and then treated with 20 μM Y27632 for 48 h. After fixation with alcohol, cells were re-suspended in 1 ml of fluorochrome solution (propidium iodide at 0.05 mg/ml with 0.1 mg/ml RNAase) and incubated at 37 °C for 1 h in the dark. Thereafter, 2.0×10^4 cells per sample were collected for analysis using flow cytometry (BD BioSciences). Cell cycle status was quantified using the software Flowjo 7.6 Tree Star Inc. (Ashland, OR, USA).

siRNA molecule transfection

Two sets of pre-validated siRNA molecules (Qiagen, Hilden, Germany) were used to target different regions of ROCK mRNA. PC3 cells were transfected with siRNA molecules and non-target siRNAs (the scrambled control) using siPORTTM NeoFXTM Transfection Agent (Ambion Inc., Austin, TX, USA) following the manufacturer's instructions. The experiments were performed 48 h after transfection.

ROCK kinase activity assay

PC3 cells were treated with 10 or 20 μM Y27632 in culture medium with 1% FBS for 48 h. After washing with cold PBS, cells were lysed with the lysis buffer and the supernatants were obtained after centrifugation. ROCK kinase activity was determined by the ROCK Activity Assay kit (Millipore, Bedford, MA, USA) according to the manufacturer's protocol.

Confocal laser scanning microscopy analysis of cytoskeleton

Cells were fixed with formaldehyde for 30 min and permeabilized with Triton X-100 in PBS for 5 min. Further, the cells were stained with 2 μl/ml fluorescein isothiocyanate-conjugated phalloidin (Molecular Probes, Eugene, OR, USA) and 0.2 μl/ml 4,6-diamidino-2-phenylindole (Molecular Probes) for 30 min in the dark after blocking with 1% fetal calf serum. Laser scanning confocal microscopy was then carried out to image the cells.

Immunofluorescent staining of p-c-Myc

PC3 cells were cultured in medium containing 1% FBS with or without 20 μM Y27632 for 48 h. Thereafter, cells were fixed with formaldehyde followed by remobilization with Triton X-100. Immunofluorescence study was carried out according to the standard procedures.[43] Briefly, the cells were blocked for 1 h with 1% fetal calf serum in PBS. Cells were incubated for 2 h at room temperature with anti-p-c-Myc polyclonal antibody (1:200, Santa Cruz Biotechnology, Santa Cruz, CA, USA). The cells were then washed three times with PBS followed by incubation with dylight 594-affinipure goat anti-rabbit immunoglobulin G secondary antibody (EarthOx, LLC, San Francisco, CA, USA) for 1 h. After washing with PBS, the cells were examined under a Confocal laser-scanning microscope. Fluorescein isothiocyanate-conjugated phalloidin was used to label cellular F-actin, and cell nuclei were counterstained with 4,6-diamidino-2-phenylindole.

Transwell migration assay

First, 100 μl of diluted matrigel was loaded onto the upper chambers of 24-well transwells and incubated at 37 °C for 6 h. PC3 cells were treated with 10 or 20 μM Y27632 or transfected with siRNA molecules for 48 h, and cell motility was assessed with the transwell migration assay. A total of 1.0×10^4 cells in 100 μl medium were seeded onto the upper chambers in 3–4 replicates under a chemotactic gradient of serum. After the cells were cultured at 37 °C overnight, the filters were removed and fixed with formaldehyde and then stained with 0.2 μl/ml 4,6-diamidino-2-phenylindole

solution. The cell nuclei on the filters were visualized under a fluorescent microscope.

Bead-based cell migration assay

The *in vitro* migration of PC3 cells was further evaluated using Cytodex-1 beads. Briefly, 1.0×10^6 cells were incubated with 60 mg beads in 6 ml culture medium overnight to coat the Cytodex-1 beads. After being washed twice with the medium, the beads with PC3 cells were cultured in medium containing 1% FBS with or without 10 or 20 μM Y27632. After 48 h, the beads were washed off and the cells that had migrated to the bottom of each well were stained with Giemsa, followed by visualization under a microscope.

Mutagenesis on S62 of c-Myc

Mutagenesis of Ser62 (S62) to Ala (A) of c-Myc protein was performed with the PCR-based QuikChange II Site-Directed Mutagenesis Kit (Agilent Technologies, Palo Alto, CA, USA), according to the instructions from the manufacturer. PCR primers were as follows: forward, 5′-CTGCTGCCCACCCCGCCCCTGGCCCCTAGCCGCCGCTCCGGGCTC-3′; reverse, 5′-GAGCCCGGAGCGGCGGCTAGGGGCCAGGGGCGGGGTGGGCAGCAG-3′.
Wt or mutant c-Myc complementary DNA was constructed into the pCMV-Tag2 expression vector. Plasmid DNA was transfected into PC3 cells using Lipofectamine 2000 (Invitrogen, Carlsbad, CA, USA) following a standard protocol provided by the manufacturer. The cells were washed with cold PBS and collected into lysis buffer 48 h after transfection, and western blotting was then performed.

Quantitative reverse transcriptase–PCR analysis

Total RNAs were isolated from cells using Trizol (Invitrogen) following the manufacturer's instructions. Quantitative measurements of gene expression were recorded with DNA Engine Opticon 2 (Bio-Rad, Richmond, CA, USA) equipped with Opticon Monitor 2 software (MJ Research, Waltham, MA, USA). Glyceraldehyde 3-phosphate dehydrogenase was used as the internal control. The primer sequences for genes in quantitative reverse transcriptase–PCR analysis are presented in Supplementary Table 2.

Quantification of western blots and reverse transcriptase–PCR images

The intensities of autoradiograms in western blots and PCR bands in agarose gels were quantified with Image J (NIH, http://rsbweb.nih.gov), and the quantified data of each gene/protein/miRNA were normalized to those of glyceraldehyde 3-phosphate dehydrogenase.

Statistical analysis

The two-tailed Student *t*-test was used to analyze the experimental data. Data are shown as mean ± s.e. $P < 0.05$ was considered statistically significant.

CONFLICT OF INTEREST

The authors declare no conflict of interest.

ACKNOWLEDGEMENTS

This work was supported by the National Natural Science Foundation of China (grant numbers: 21377159, 81172451) and from the national '973' program (grant number: 2014CB932000). We thank lab members for their invaluable assistance with experiments and reagents, and Michael Rosenblatt, MD, of Merck & Co. Inc. for his review of the manuscript and helpful suggestions.

REFERENCES

1 Narumiya S, Tanji M, Ishizaki T. Rho signaling, ROCK and mDia1, in transformation, metastasis and invasion. *Cancer Metastasis Rev* 2009; **28**: 65–76.
2 Hahmann C, Schroeter T. Rho-kinase inhibitors as therapeutics: from pan inhibition to isoform selectivity. *Cell Mol Life Sci* 2010; **67**: 171–177.
3 Bu QTH, Tan J, Hu X, Wang DW. Expression of RhoC and ROCK-1 and their effects on MAPK and Akt proteins in prostate carcinoma. *Chin J Oncol* 2011; **33**: 202–206.
4 Liu S. The ROCK signaling and breast cancer metastasis. *Mol Biol Rep* 2011; **38**: 1363–1366.
5 James K, Liao MS, Noma K. Rho kinase (ROCK) inhibitors. *J Cardiovasc Pharmacol* 2007; **50**: 17–24.
6 Nakagawa O, Fujisawa K, Ishizaki T, Saito Y, Nakao K, Narumiya S. ROCK-I and ROCK-II, two isoforms of Rho-associated coiled-coil forming protein serine/threonine kinase in mice. *FEBS Lett* 1996; **392**: 189–193.
7 Riento K, Totty N, Villalonga P, Garg R, Guasch R, Ridley AJ. RhoE function is regulated by ROCK I-mediated phosphorylation. *EMBO J* 2005; **24**: 1170–1180.
8 Zhang Y, Li X, Qi J, Wang J, Liu X, Zhang H *et al.* Rock2 controls TGFβ signaling and inhibits mesoderm induction in zebrafish embryos. *J Cell Sci* 2009; **122**: 2197–2207.
9 Lochhead PA, Wickman G, Mezna M, Olson MF. Activating ROCK1 somatic mutations in human cancer. *Oncogene* 2010; **29**: 2591–2598.
10 Liu S, Goldstein RH, Scepansky EM, Rosenblatt M. Inhibition of Rho-associated kinase signaling prevents breast cancer metastasis to human bone. *Cancer Res* 2009; **69**: 8742–8751.
11 Lane J, Martin TA, Watkins G, Mansel RE, Jiang WG. The expression and prognostic value of ROCK I and ROCK II and their role in human breast cancer. *Int J Oncol* 2008; **33**: 585–593.
12 Lin S-L, Chang D, Ying S-Y. Hyaluronan stimulates transformation of androgen-independent prostate cancer. *Carcinogenesis* 2006; **28**: 310–320.
13 Routhier A, Lahey D, Monfredo N, Johnson A, Callahan W, Partington A *et al.* Pharmacological inhibition of Rho-kinase signaling with Y-27632 blocks melanoma tumor growth. *Oncogene Rep* 2010; **23**: 861–867.
14 Dang CV, O'Donnell KA, Zeller KI, Nguyen T, Osthus RC, Li F. The c-Myc target gene network. *Sem Cancer Biol* 2006; **16**: 253–264.
15 Wang C, Lisanti MP, Liao DJ. Reviewing once more the c-myc and Ras collaboration: converging at the cyclin D1-CDK4 complex and challenging basic concepts of cancer biology. *Cell Cycle* 2011; **10**: 57–67.
16 Hann SR. Role of post-translational modifications in regulating c-Myc proteolysis, transcriptional activity and biological function. *Sem Cancer Biol* 2006; **16**: 288–302.
17 Watnick RS, Cheng Y-N, Rangarajan A, Ince TA, Weinberg RA. Ras modulates Myc activity to repress thrombospondin-1 expression and increase tumor angiogenesis. *Cancer Cell* 2003; **3**: 219–231.
18 Itoh K, Yoshioka K, Akedo H, Uehata M, Ishizaki T, Narumiya S. An essential part for Rho-associated kinase in the transcellular invasion of tumor cells. *Nat Med* 1999; **5**: 221–225.
19 Uehata M, Ishizaki T, Satoh H, Ono T, Kawahara T, Morishita T *et al.* Calcium sensitization of smooth muscle mediated by a Rho-associated protein kinase in hypertension. *Nature* 1997; **389**: 990–994.
20 Chan CH, Lee SW, Li CF, Wang J, Yang WL, Wu CY *et al.* Deciphering the transcriptional complex critical for RhoA gene expression and cancer metastasis. *Nat Cell Biol* 2010; **12**: 457–467.
21 Noguchi K, Kokubu A, Kitanaka C, Ichijo H, Kuchino Y. ASK1-signaling promotes c-Myc protein stability during apoptosis. *Biochem Biophys Res Commun* 2001; **281**: 1313–1320.
22 Alarcon-Vargas D, Ronai Z. c-Jun-NH2 kinase (JNK) contributes to the regulation of c-Myc protein stability. *J Biol Chem* 2004; **279**: 5008–5016.
23 Alarcon-Vargas D, Tansey WP, Ronai Z. Regulation of c-myc stability by selective stress conditions and by MEKK1 requires aa 127-189 of c-myc. *Oncogene* 2002; **21**: 4384–4391.
24 Kenney AM, Widlund HR, Rowitch DH. Hedgehog and PI-3 kinase signaling converge on Nmyc1 to promote cell cycle progression in cerebellar neuronal precursors. *Development* 2004; **131**: 217–228.
25 Seth A, Gupta S, Davis RJ. Cell cycle regulation of the c-Myc transcriptional activation domain. *Mol Cell Biol* 1993; **13**: 4125–4136.
26 Luscher B, Eisenman RN. Mitosis-specific phosphorylation of the nuclear oncoproteins Myc and Myb. *J Cell Biol* 1992; **118**: 775–784.
27 Butt A, Sergio CM, Inman C, Anderson L, McNeil C, Russell A *et al.* The estrogen and c-Myc target gene HSPC111 is over-expressed in breast cancer and associated with poor patient outcome. *Breast Cancer Res* 2008; **10**: R28.
28 Krutzfeldt J, Rajewsky N, Braich R, Rajeev KG, Tuschl T, Manoharan M *et al.* Silencing of microRNAs in vivo with /'antagomirs/'. *Nature* 2005; **438**: 685–689.
29 Hesan Luo JZ, Dong Z, Zeng Q, Wu D, Liu L. Up-regulated miR-17 promotes cell proliferation, tumour growth and cell cycle progression by targeting the RND3 tumour suppressor gene in colorectal carcinoma. *Biochem J* 2012; **442**: 311–321.
30 Boku S, Nakagawa S, Toda H, Kato A, Takamura N, Omiya Y *et al.* ROCK2 regulates bFGF-induced proliferation of SH-SY5Y cells through GSK-3β and β-catenin pathway. *Brain Res* 2013; **1492**: 7–17.
31 Yeh E, Cunningham M, Arnold H, Chasse D, Monteith T, Ivaldi G *et al.* A signalling pathway controlling c-Myc degradation that impacts oncogenic transformation of human cells. *Nat Cell Biol* 2004; **6**: 308–318.

32 Gualco G WL, Harrington Jr WJ, Bacchi CE. Nodal diffuse large B-cell lymphomas in children and adolescents: immunohistochemical expression patterns and c-MYC translocation in relation to clinical outcome. *Am J Surg Pathol* 2009; **33**: 1815–1822.
33 Ruzinova MB CT, Rodig SJ. Altered subcellular localization of c-Myc protein identifies aggressive B-cell lymphomas harboring a c-MYC translocation. *Am J Surg Pathol* 2010; **34**: 882–891.
34 Alvarez E, Northwood IC, Gonzalez FA, Latour DA, Seth A, Abate C *et al.* Pro-Leu-Ser/Thr-Pro is a consensus primary sequence for substrate protein phosphorylation. Characterization of the phosphorylation of c-myc and c-jun proteins by an epidermal growth factor receptor threonine 669 protein kinase. *J Biol Chem* 1991; **266**: 15277–15285.
35 Seth A, Alvarez E, Gupta S, Davis RJ. A phosphorylation site located in the NH2-terminal domain of c-Myc increases transactivation of gene expression. *J Biol Chem* 1991; **266**: 23521–23524.
36 Sears RC. The life cycle of C-myc: from synthesis to degradation. *Cell Cycle* 2004; **3**: 1133–1137.
37 Welcker M, Orian A, Grim JA, Eisenman RN, Clurman BE. A nucleolar isoform of the Fbw7 ubiquitin ligase regulates c-Myc and cell size. *Curr Biol* 2004; **14**: 1852–1857.
38 Welcker M, Orian A, Jin J, Grim JA, Harper JW, Eisenman RN *et al.* The Fbw7 tumor suppressor regulates glycogen synthase kinase 3 phosphorylation-dependent c-Myc protein degradation. *Proc Natl Acad Sci USA* 2004; **101**: 9085–9090.
39 Popov N, Herold S, Llamazares M, Schulein C, Eilers M. Fbw7 and Usp28 regulate myc protein stability in response to DNA damage. *Cell Cycle* 2007; **6**: 2327–2331.
40 Liu S, Li S, Du Y. Polychlorinated biphenyls (PCBs) enhance metastatic properties of breast cancer cells by activating Rho-associated kinase (ROCK). *PLoS One* 2010; **5**: e11272.
41 Fontana L, Fiori ME, Albini S, Cifaldi L, Giovinazzi S, Forloni M *et al.* Antagomir-17-5p abolishes the growth of therapy-resistant neuroblastoma through p21 and BIM. *PLoS One* 2008; **3**: e2236.
42 Taylor BS, Schultz N, Hieronymus H, Gopalan A, Xiao Y, Carver BS *et al.* Integrative genomic profiling of human prostate cancer. *Cancer Cell* 2010; **18**: 11–22.
43 Liu S, RNVS Suragani, Wang F, Han A, Zhao W, Andrews NC *et al.* The function of heme-regulated eIF2α kinase in murine iron homeostasis and macrophage maturation. *J Clin Investig* 2007; **117**: 3296–3305.

Supplementary Information accompanies this paper on the Oncogene website (http://www.nature.com/onc)